Three-Arm Poly(dimethylsiloxane) Junction Bearing a Single Pendant Dansyl Group: A Model Architecture for Polymer Junction Points Dissolved in Liquids and Molten Polymers

Chase A. Munson, Maureen A. Kane, Gary A. Baker, Siddharth Pandey,† Sherryl A. Perez, and Frank V. Bright*

Department of Chemistry, Natural Sciences Complex, University at Buffalo, The State University of New York, Buffalo, New York 14260-3000

Received January 3, 2001; Revised Manuscript Received April 23, 2001

ABSTRACT: We have determined the static and time-resolved fluorescence of a poly(dimethylsiloxane) (PDMS)-based three-armed junction that contains a single dansyl reporter group when it is dissolved at low concentration in three normal liquids (good, Θ, and poor solvents) and neat methyl-terminated PDMS. The junction results are compared to a "junctionless" analogue—dansyl propylamine. We report on the activation energies for dansyl thermal quenching and rotational reorientation and the dansyl residue's ability to reorient and precess at the junction point. In normal liquids a decrease in solvent quality leads to a collapse of the junction's PDMS arms around the dansyl reporter group, an inhibition of the dansyl residue's ability to form its twisted intramolecular charge transfer state, and impedance of the dansyl residue's ability to reorient. When the junction is dissolved in neat methyl-terminated PDMS, there is evidence for chain-length-dependent interpenetration of the PDMS "solvent" molecules into the junction and modulation of the local microenvironment surrounding the dansyl residue at the junction. These results demonstrate the dramatic role solvent can play in tuning the local microenvironment that surrounds a polymeric junction point.

Introduction

Polymer chains can undergo random Brownian motion induced by local conformational transitions of the polymer backbone or side chains.[1] These dynamics are governed by the polymer structure itself and, in dilute solution, the solvent physicochemical properties (viscosity, dipolarity, temperature). The impact of these factors controls the use of polymers in packaging,[2] drug delivery,[3] and nonlinear optics.[4] The ability to control the mechanical, rheological, and related polymer properties through the synthesis of complex macromolecular architectures is also central to a number of other research activities.[5]

Polymer dynamics have been studied by a number of methods including, neutron scattering,[6] nuclear magnetic resonance spectroscopy,[7] electron spin resonance spectroscopy,[8] dielectric relaxation,[9] dynamic light scattering,[10] and fluorescence spectroscopy.[11] Fluorescence is a useful tool for assessing the local microenvironment that surrounds a fluorescent probe molecule (i.e., the cybotactic region), for exploring the polymer dynamics on a nanosecond and subnanosecond time scale, and for studying dilute polymer solutions, polymer melts and blends, and entangled or cross-linked polymer networks.[11,12] In these types of experiments, the fluorescence can arise from an intrinsic fluorophore that is part of the polymer (e.g., the benzene ring in poly(styrene)), or it derives from an extrinsic probe. Extrinsic probes can be randomly dispersed within a polymer sample, or they can be attached by covalent bonds to specific sites within the polymer. The primary advantage of the covalent attachment strategy lies in the probe molecule being located at a specific site within the polymer at all times regardless of the system variables.

Previous work by the Frank and Fayer groups investigated the dynamics of probe-labeled poly(dimethylsiloxane) (PDMS) junctions that were part of larger networks.[12] These networks were prepared by a condensation reaction between OH-terminated PDMS (HO−PDMS−OH) and a mixture of dansyltriethoxysilane (DTES) and methyltriethoxysilane (MTES). When these authors recorded the time-resolved fluorescence anisotropy decay of the dansyl fluorophore in these networks, they discovered that the dansyl residue exhibited nanosecond and subnanosecond rotational reorientation dynamics within these macroscopically solid PDMS networks. Unfortunately, these particular networks are extremely complex because the cross-linking efficiency is not 100%, and each dansyl residue does not encounter the exact same microenvironment because DTES can hydrolyze and condense with other DTES molecules, with MTES, and/or with HO−PDMS−OH.[13]

The current work focuses on the behavior of a well-defined polymer junction that has a single fluorescent probe molecule located at the junction. Specifically, we report on the behavior of a PDMS-based, three-armed junction that contains a single dansyl reporter group—the dansyl junction, DJ. We compare our results to the same system without a junction—dansyl propylamine (DPA). The DPA and DJ structures are shown in Figure 1. We have investigated the static and time-resolved fluorescence from DPA and DJ when they are dissolved at low concentration (<10 μM) in three normal liquids (toluene, ethyl acetate, and methanol) and in three, linear methyl-terminated PDMS polymers (2.0, 3.8, and 28 kDa). The goals of these experiments are to determine how solvent quality (good, Θ, and poor), polymer molecular weight, and temperature influence the junc-

† Current address: Department of Chemistry, New Mexico Tech, Socorro, NM 87801.

* To whom all correspondence should be directed: (716) 645-6800 ext 2162 (voice), (716) 645-6963 (Fax), chefvb@acsu.buffalo.edu (e-mail).

10.1021/ma010013c CCC: $20.00
Published on Web 05/22/2001

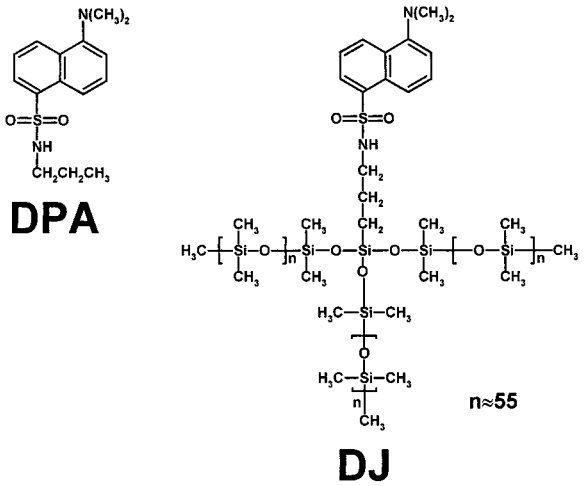

Figure 1. Chemical structures of the species investigated: dansyl propylamine (DPA) and three-arm PDMS junction bearing a single pendant dansyl residue (DJ).

tion. Dansyl was chosen as our fluorescent probe because its static and time-resolved fluorescence are sensitive to subtle changes in its cybotactic region.[14]

Theory Section

The theory of frequency-domain fluorescence for recovering the fluorescence anisotropy and intensity decay kinetics has been reviewed elsewhere.[15] Briefly, a sample is excited with sinusoidally modulated light, and the experimental measurables are the frequency-dependent phase angle (Θ_ω) and demodulation factor (M_ω) for the excited-state fluorescence intensity decay or the differential polarized phase angle (Λ_ω) and polarized modulation ratio (Δ_ω) for the fluorescence anisotropy decay.

Excited-State Intensity Decay Kinetics. Θ_ω and M_ω data are used to recover the time-resolved fluorescence intensity decay $I(t)$.[14,15] $I(t)$ is typically described by[15,16]

$$I(t) = \sum_{i=1}^{N} f_i \exp(-t/\tau_i) \tag{1}$$

In this expression, f_i and τ_i represent the apparent fractional intensity and excited-state fluorescence lifetime, respectively, of the ith emissive species. The average excited-state fluorescence lifetime $\langle\tau\rangle$ is expressed as

$$\langle\tau\rangle = \sum_{i=1}^{N} f_i\tau_i \tag{2}$$

Time-Resolved Anisotropy Decay Kinetics. Λ_ω and Δ_ω data are used to recover the time-resolved fluorescence anisotropy decay $r(t)$ of a fluorophore.[15,16] For fluorescent probes bound to a polymer network, $r(t)$ frequently involves a superposition of two discrete motions.[11] If we consider a single fluorescent probe that is covalently attached to a larger species that itself undergoes isotropic rotational diffusion and we assume independent local probe rotational reorientation, $r(t)$ can be approximated by[15,17]

$$r(t) = r_0[A \exp(-\tau/\phi_{\text{fast}}) + (1 - A) \exp(-t/\phi_{\text{slow}})] \tag{3}$$

where r_0 is the fluorophore's limiting anisotropy, A is the fractional contribution to the total anisotropy decay from the "fast" motion (ϕ_{fast}), and $1 - A$ is the fractional contribution to the total anisotropy decay that is attributable to the "slow" rotational reorientation (ϕ_{slow}). If the fluorophore local motion is much faster than the reorientation for the entire adduct (i.e., $\phi_{\text{fast}} \ll \phi_{\text{slow}}$), the *true* fluorophore local motion $\phi_{\text{fast(true)}}$ is given by[17]

$$\frac{1}{\phi_{\text{fast(true)}}} = \frac{1}{\phi_{\text{fast}}} - \frac{1}{\phi_{\text{slow}}} \tag{4}$$

If the local fluorophore reorientation is independent of the adduct global motion, one can associate the fluorophore's ability to precess or reorient during its excited-state fluorescence lifetime with a semiangle (θ_0):[17]

$$\theta_0 = \cos^{-1}\left[\frac{1}{2}((8(1 - A)^{1/2} + 1)^{1/2} - 1)\right] \tag{5}$$

Within this "wobbling-in-a-cone" model, the fluorophore can only reorient within a conical subdomain that is defined by θ_0. Thus, if θ_0 approaches 0°, the fluororophore local motion becomes completely restricted ($A = 0$). In contrast, complete freedom to precess/reorient within the probe's cybotactic region ($A = 1$) is associated with a θ_0 of 90°.

For small values of θ_0, Lipari and Szabo[17b] have shown that one can assign a wobbling diffusion coefficient D_w to the fluorophore's precession:

$$D_w = \frac{7\theta_0^2}{24\phi_{\text{fast(true)}}} \tag{6}$$

For $\theta_0 = 30°$, the error in D_w is reportedly less than 10%.[17b] (Note: the units for θ_0 in eq 6 are radians.)

Stokes Shifts. The Stokes shift (SS, difference between the electronic absorbance and emission maxima in cm^{-1}) for a solvatochromic fluorophore depends on the solvent's dielectric constant (ϵ) and refractive index (n) through the Lippert−Mataga expression:[18]

$$\text{SS} = \frac{\Delta f}{hca^3}(\mu_E - \mu_G)^2 + \text{constant} \tag{7}$$

where h is Planck's constant, c is the speed of light, a is the cavity radius swept out by the fluorophore, μ_E is the fluorophore excited-state dipole moment, μ_G is the fluorophore ground-state dipole moment, and Δf is the solvent orientational polarizability, is given as

$$\Delta f = [(\epsilon - 1)/(2\epsilon + 1)] - [(n^2 - 1)/(2n^2 + 1)] \tag{8}$$

Experimental Section

Reagents. The following were used: HPLC grade toluene, HPLC grade ethyl acetate, dansyl chloride, propylamine, 1,4-bis(4-methyl-5-phenyl-2-oxazolyl)benzene (Me_2POPOP) (Aldrich); spectrophotometric grade methanol (Sigma); and ethanol (dehydrated, 200 proof) (Pharmco). Methyl-terminated PDMS polymers having molecular weights of 2.0, 3.8, and 28 kDa were obtained from United Chemical Technologies.

Three-Arm Junction Synthesis. A three-arm PDMS-based polymer junction bearing a single dansyl fluorophore (DJ in Figure 1) was custom synthesized by Polymer Source Inc. The synthesis involved the anionic polymerization of hexamethylcyclotrisiloxane followed by termination with purified DTES. The desired product was separated from undesired species (two-arm polymer and unreacted DTES) by using a toluene/methanol fractionation step. Gel permeation chroma-

tography showed that the final DJ exhibited the following characteristics: $M_w \sim 15\,000$ and $M_w/M_n = 1.20$.

Dansylpropylamine (DPA) Synthesis. Dansyl chloride was reacted under ambient conditions with a 25-fold molar excess of neat propylamine for a period of 1 week at room temperature in the dark. Propylamine was removed by evaporation with a stream of N_2, leaving behind crude DPA. The crude DPA was purified by column chromatography.

Fluorescence Experiments. All fluorescence experiments were performed by using an SLM-AMINCO model 48000 MHF (Spectronic Instruments). For static fluorescence measurements, a 450 W xenon arc lamp was used for excitation and single grating monochromators served as the wavelength selection devices. The excitation and emission spectral bandpasses were maintained at 4 nm, and all emission spectra were background corrected by using appropriate blanks. The blank contribution was always less than 0.5% of the total emission.

The time-resolved fluorescence anisotropy and intensity decay kinetics were measured in the frequency domain by using the 48000 MHF. For these particular experiments we used a CW argon ion laser (Coherent, Innova 90-6) operating at 363.8 nm as the excitation source. An interference filter (Oriel) was placed in the excitation beam path to minimize extraneous plasma tube superradiance from reaching the emission detection system. The entire dansyl fluorescence was monitored by using a 420 nm long-pass filter (Oriel). The Pockels cell modulator was operated at a 5 MHz base repetition rate. Typically, data were acquired for 60 s between 5 and 200 MHz at 5 MHz intervals, and we acquired at least 10 discrete multifrequency data sets for each sample under a given set of experimental conditions. For the excited-state intensity decay measurements, we used a dilute solution of Me_2POPOP dissolved in ethanol as the reference lifetime standard; its lifetime was assigned a value of 1.45 ns. Magic angle polarization conditions[19] were used for all excited-state intensity decay measurements to eliminate bias arising from fluorophore rotational reorientation. The excited-state intensity decay kinetics and rotational reorientation times were recovered from the frequency-domain data by using a commercially available, nonlinear least-squares software package (Globals Unlimited). We used the frequency-dependent experimental uncertainty in each datum as our weighting factors.

The sample temperature was controlled to within 0.1 °C by using a circulating water bath (VWR model 1140). The sample temperature was determined within the sample cuvette by a solid-state thermocouple (Cole Parmer, model 8517-00).

Statistics. All results are the average of at least three separate experiments. Results are reported as the average for a series of experiments under a given set of conditions. All error bars represent ±1 standard deviation.

Results and Discussion

Steady-State Fluorescence from DJ and DPA. Toluene, ethyl acetate (EtAc), and methanol (MeOH) were selected as solvents because they are good, Θ, and poor solvents for PDMS, respectively.[20] Within a good solvent, a linear polymer should be extended because the segments interact favorably with the solvent more so than they do with themselves. In a poor solvent, a polymer will collapse upon itself because the segment−solvent interactions are less favorable in comparison to the segment−segment interactions. A Θ solvent exhibits characteristics that are intermediate between good and poor solvents. In a Θ solvent below the Θ temperature, a polymer behaves as if it is dissolved in a poor solvent. Above the Θ temperature, the polymer should behave as if it were dissolved in a good solvent. For PDMS dissolved in EtAc, the Θ temperature occurs at 4.8 °C.[20]

We found that the dansyl Stokes shifts were not particularly temperature dependent in a given solvent between −10 and +50 °C. Thus, we used the average Stokes shifts across this temperature range to initially assess the dansyl probe's cybotactic region. Figure 2 presents the average DPA and DJ Stokes shifts in toluene, EtAc, MeOH, and the 2, 3.8, and 28 kDa PDMS polymers. In the three liquids, the DPA Stokes shift is always greater than the corresponding DJ Stokes shift. Thus, the PDMS arms on DJ clearly interact to some extent with the dansyl chromophore (i.e., regardless of solvent the dansyl "sees and feels" the junction's PDMS arms). Because the PDMS is less dipolar compared to these solvents, this interaction is manifest in a decrease in the DJ Stokes shift relative to DPA. Also, because DPA has no "arms" to interact with, its behavior depends only on the solvent dipolarity. The DPA Stokes shift in the most dipolar solvent (MeOH) is the largest, and it is the smallest in the least dipolar solvent (toluene) (eqs 7 and 8).

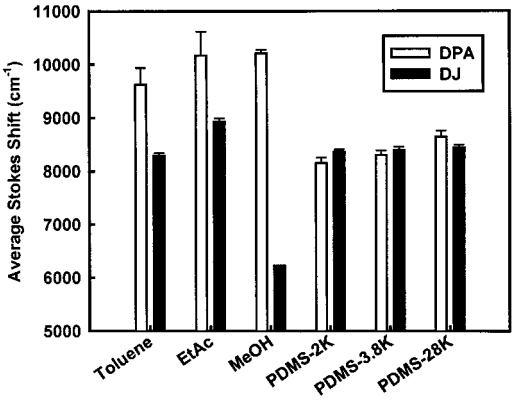

Figure 2. Average Stokes shifts for DPA (□) and DJ (■) dissolved in normal liquids and methyl-terminated PDMS.

The results for DJ dissolved in MeOH are especially dramatic. On the basis of the relative solvent orientational polarizability (eq 8), one would predict that the Stokes shift for DJ dissolved in MeOH should exhibit shifts greater than those observed for DJ dissolved in EtAc and toluene. However, Figure 2 clearly shows this not to be the case, and the DJ Stokes shift in MeOH is much less than the Stokes shift for either DJ or DPA dissolved in neat PDMS. MeOH is a poor solvent for PDMS;[20] therefore, it is likely that the PDMS arms on DJ, in MeOH, collapse around the dansyl fluorophore, sequestering the dansyl reporter group within a PDMS-rich environment. But, why then is the Stokes shift for DJ dissolved in MeOH even less than that for DJ or DPA dissolved in neat PDMS?

Molecules like dansyl exhibit solvatochromic behavior for at least two reasons.[21] First, they exhibit general solvent effects that arise from the fluorophore's change in dipole moment upon optical excitation and the solvent's dielectric constant and refractive index as described by the Lippert−Mataga expression (eq 7). Second, a portion of their solvatochromism arises from the fact that they possess two excited states: locally excited (LE) and twisted intramolecular charge transfer (TICT). Upon optical excitation the less polar, semiplanar LE state forms initially (similar in structure to the ground state) which can undergo intramolecular electron transfer from a donor residue ($-N-(CH_3)_2$ in dansyl) to an acceptor with a corresponding twist of the donor residue about the bond that connects it to the acceptor. In the TICT state, the donor and acceptor are orthogonal to one another, and this state is much more polar in comparison to the LE state. Thus, the propensity to form the TICT state and thus shift the spectrum

is influenced by the solvent dielectric properties which helps to mediate charge transfer *and* the ability of the donor residue to rotate within the fluorophore. The former is governed primarily by the solvent dielectric properties, and the latter depends also on any physical impediments to donor rotation. We suggest that the reason for the DJ Stokes shift in MeOH being less than DJ in neat PDMS arises from a physical blocking of the $-N-(CH_3)_2$ residue from reorienting due to the collapsing PDMS arms on DJ.

The right half of Figure 2 summarizes the behavior of DPA and DJ dissolved in 2, 3.8, and 28 kDa PDMS. These results are less dramatic than the results seen in the liquids; however, given the measurement precision, there are some notable trends. As the PDMS solvent molecular weight increases, there is a modest increase in the DPA Stokes shift. This result suggests that the DPA is seeking out and/or locating within a cybotactic region that is progressively more dipolar as the PDMS chain length increases. We assign this shift to a decrease in relative contribution from PDMS chain termini ($Si-(CH_3)_3$)/dansyl interactions and an increase in chain core (($-O-Si(Me)_2-O-$)/dansyl interactions with increasing PDMS molecular weight. The DJ Stokes shift in the three PDMS samples remains essentially constant with PDMS molecular weight.

When we compare the DJ/PDMS and DPA/PDMS results to one another, we note the following trends. In the 2 kDa PDMS, the dansyl residue in DJ senses a more dipolar environment compared to DPA. The dansyl residues in DJ and DPA encounter equivalent environments in the 3.8 kDa PDMS samples. The dansyl residue in DJ dissolved in the 28 kDa PDMS senses an environment that is less dipolar compared to that surrounding DPA. One possible explanation for these results involves the relative length scales of the PDMS solvent chains compared to the DJ arm length. For example, the 2 kDa PDMS chains are about half the DJ arm length, the 3.8 kDa PDMS is nearly the same length as a DJ arm, and the 28 kDa PDMS is substantially longer than the DJ arm. Given this, one can envision the 2 kDa PDMS associating fully with the extended DJ arms, but the short PDMS length precludes the less dipolar PDMS chain termini of the 2 kDa polymer from accessing the dansyl residue within DJ. The 3.8 kDa PDMS might associate completely with the DJ arms, and the PDMS chain termini could access the dansyl residue. The 28 kDa polymer is so long that both termini of a single PDMS chain could access the dansyl residue within DJ.

Time-Resolved Intensity Decay Studies. The $I(t)$ that describes the DJ and DPA behavior are described by a biexponential decay model in all samples and under all conditions we investigated. In general, $I(t)$ is characterized by a 12−14 ns ($T = 0$ °C) component (τ_1) that comprises about 90% (50% in MeOH) of the intensity decay. The second decay time (τ_2) lies in the 1−4 ns range. These results are fully consistent with a system that exhibits emission from LE and TICT states.[21]

The temperature dependence of $\langle\tau\rangle$ follows an Arrhenius-type behavior between 0 and 40 °C (r^2 for all Arrhenius plots > 0.94). The recovered activation energies for DJ and DPA thermal quenching ($E_{a,TQ}$) in the liquids and PDMS are depicted in Figure 3. In the liquids the recovered $E_{a,TQ}$ values for DJ increase significantly as we progress from toluene to EtAc to MeOH (i.e., good to Θ to poor solvent). Thus, for DJ a

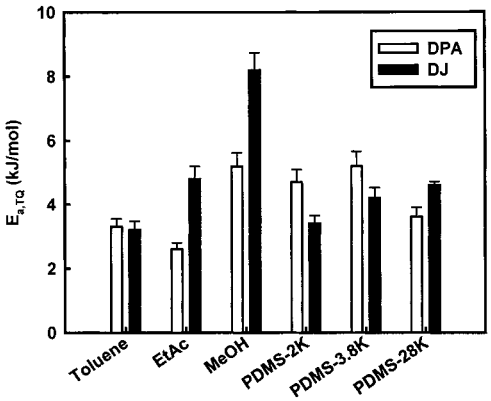

Figure 3. Activation energies for thermal quenching for DPA and DJ dissolved in normal liquids and methyl-terminated PDMS.

decrease in solvent quality leads to a concomitant increase in $E_{a,TQ}$. This result is consistent with the DJ arms progressively closing in about the dansyl residue as we move from a good to Θ to poor solvent, and the "closed in" arms in effect insulate the dansyl residue from thermal quenching processes. In comparing DJ and DPA dissolved in each liquid, we see that the $E_{a,TQ}$ values are equivalent in toluene, suggesting that the insulating power of the DJ arms in a good solvent is minimal. This result is expected if the PDMS arms on DJ are extended in toluene. As we proceed to the Θ solvent (EtAc), we see that more energy is required to quench DJ compared to DPA. This result argues that the PDMS arms in DJ are offering some protection to dansyl residue in DJ relative to DPA dissolved in EtAc. Finally, in the poor solvent (MeOH), slightly more energy (relative to the EtAc system) is required to quench DJ compared to DPA. This result argues that the PDMS arms in DJ are offering greater protection to the dansyl residue in DJ when it is dissolved in MeOH relative to DPA dissolved in MeOH.

When DJ and DPA are dissolved in PDMS, the differences between the two species are less striking. For DJ there is a systematic increase in $E_{a,TQ}$ as we increase the PDMS chain length. This result is in line with our hypothesis involving differences in the PDMS solvent chains being able to penetrate in along the PDMS arms and access the dansyl residue in DJ. The shorter PDMS chains offer less insulating ability relative to the longer PDMS chains. A comparison of DJ and DPA to one another in each PDMS solvent show an interesting trend. First, in the 2 kDa PDMS, more energy is required to quench DPA compared to DJ. This result is consistent with DPA being more insulated and the dansyl residue in DJ being less insulated by the 2 kDa PDMS. Second, in the 3.8 kDa PDMS, additional energy is required to quench DPA compared to DJ, but this energy is less than the extra energy required in the 2 kDa PDMS. This result is consistent with DPA being more insulated and the dansyl residue in DJ being a bit more insulated by the 3.8 kDa PDMS chains. Third, in the 28 kDa PDMS, less energy is required to quench DPA compared to DJ. This result is consistent with DPA being less well insulated and the dansyl residue in DJ being more insulated by the 28 kDa PDMS chains. Together these results are in line with our PDMS "solvent" chain penetration argument (vide supra).

Time-Resolved Anisotropy Decay Studies. The $r(t)$ for DJ and DPA dissolved in the liquids is described

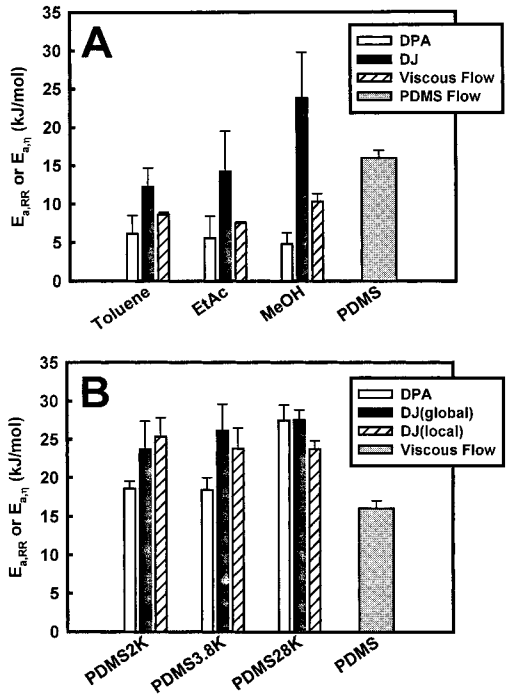

Figure 4. Comparison of the activation energies for dansyl residue rotational reorientation and solvent/PDMS viscous flow: (A) DPA and DJ dissolved in normal liquids; (B) DPA and DJ dissolved in methyl-terminated PDMS.

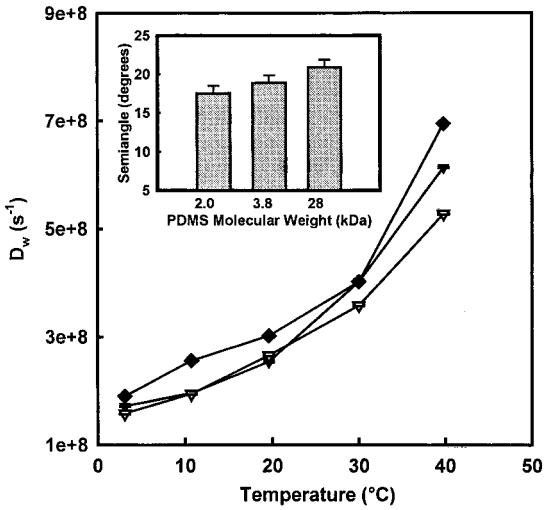

Figure 5. Dansyl residue within DJ wobbling diffusion constant (D_w) as a function of sample temperature in 2 (□), 3.8 (▽), and 28 kDa (◆) methyl-terminated PDMS. (inset) Dansyl residue semiangle as a function of PDMS molecular weight.

by a single-exponential decay model (i.e., isotropic rotor) at all temperatures investigated. Although one might anticipate observing two rotational motions for DJ (local and global) in the liquids, we are unable to confirm this experimentally. Our inability to recover two discrete motions for DJ dissolved in liquids may arise from our lack of adequate time resolution (currently ∼40 ps). When we investigated DPA and DJ dissolved in the PDMS solvents, we found that the $r(t)$ for DPA and DJ were described by isotropic and anisotropic rotor models, respectively. Thus, we are able to detect and quantify the local and global DJ motions when it is dissolved in neat PDMS.

The temperature dependence of the DJ and DPA rotational reorientation times in the liquids and PDMS follow an Arrhenius expression (r^2 for all Arrhenius plots > 0.92). The recovered activation energies for rotational reorientation $E_{a,RR}$ are collected in Figure 4. In Figure 4A we present the $E_{a,RR}$ values for DJ and DPA dissolved in liquids along with the activation energy for solvent and PDMS viscous flow $E_{a,\eta}$. In all cases, the DPA $E_{a,RR}$ is statistically equivalent to the $E_{a,\eta}$. This is not surprising and argues that the DPA rotational reorientation is coupled purely to the solvent dynamics. The $E_{a,RR}$ for DJ is always greater than the value of DPA in the same solvent, and the DJ $E_{a,RR}$ increases systematically as we decrease the solvent quality. These results are consistent with the DJ arms impeding the dansyl residue's ability to reorient and the impediment increasing progressively as we move from a good to Θ to poor solvent. We also note that $E_{a,RR}$ for DJ dissolved in toluene and EtAc are close to the PDMS $E_{a,\eta}$. However, the $E_{a,RR}$ for DJ dissolved in MeOH exceeds $E_{a,\eta}$ for PDMS by ∼10 kJ/mol. This result argues that there is an additional energetic barrier associated with dansyl residue reorientation in DJ when it is dissolved in MeOH. This result is in line with the our steady-state results (Figure 2) where we argued that the PDMS arms on DJ collapse about the dansyl residue in the poor solvent and impede the dansyl chromophore from forming its TICT state even though the solvent per se (MeOH) is highly dipolar.

In Figure 4B we summarize the $E_{a,RR}$ values for DJ and DPA in PDMS along with the PDMS $E_{a,\eta}$. The situation here is slightly more complex because there are two rotational reorientation times for DJ dissolved in PDMS (associated with the dansyl residue's local and global motion). Inspection of Figure 4B shows several interesting trends. In the lower molecular weight PDMS samples (2 and 3.8 kDa), the $E_{a,RR}$ for DPA are roughly equivalent to the PDMS $E_{a,\eta}$. However, DPA dissolved in the 28 kDa PDMS samples exhibits an $E_{a,RR}$ that is about 50% greater than the PDMS $E_{a,\eta}$. This result argues that there is an additional mechanism to DPA reorientation in the 28 kDa PDMS samples in comparison to the 2 and 3.8 kDa PDMS samples. One possibility is that the 28 kDa PDMS sample is above the so-called entanglement molecular weight for PDMS whereas the other samples lie below the entanglement cutoff.[22]

The $E_{a,RR}$ values for DJ in each PDMS sample exhibit several interesting features. For example, the $E_{a,RR}$ values for DJ are always greater than the PDMS $E_{a,\eta}$ by ∼10 kJ/mol. These results demonstrate that there is at least one additional energy barrier to DJ reorientation in PDMS that is not accounted for by a simple PDMS viscous flow argument. As the PDMS molecular weight increases, we note that the *global* $E_{a,RR}$ for DJ increases and the *local* $E_{a,RR}$ for DJ decreases. This result argues that an increase in the PDMS chain length causes the local dansyl motion to become more facile whereas the global motion is more energetically demanding. Such a situation could be accounted for by intercalation of the PDMS solvent chains into the DJ junction and an opening up of the DJ arms. If the latter scenario were true, one would expect to see differences in the dansyl residue's freedom to reorient at the junction point.

In the inset to Figure 5, we report the dansyl residue semiangle θ_0 in DJ when it is dissolved in each PDMS sample. θ_0 clearly increases as the PDMS chain length increases in line with the PDMS solvent chains opening up the dansyl cybotactic region within the DJ. This

result is consistent with our hypothesis. The effects of temperature on the dansyl residue wobbling diffusion constant D_w are also shown in Figure 5. The most striking aspect of these data is that the dansyl residue D_w at a given temperature are remarkably similar to one another; the D_w for the DJ dissolved in the 28 kDa PDMS is, in general, greater in comparison to the 2 and 3.8 kDa samples. Together these results argue that the actual mobility of the dansyl probe per se and the domain over which the dansyl is able to reorient increase as the PDMS solvent chain length increases.

Conclusions

We have determined the static and time-resolved fluorescence of a PDMS-based, three-armed junction that contains one dansyl reporter group (DJ) at the junction when this species is dissolved at low concentration within three normal liquids (good, Θ, and poor solvents) and neat methyl-terminated PDMS. These results are compared to dansyl propylamine (DPA)—a "junctionless" analogue. The results of these experiments on DJ show that a decrease in solvent quality leads to a collapse of the PDMS arms around the dansyl reporter group, an inhibition of the dansyl LE to TICT state, and an impeding of the dansyl residue's ability to reorient. When DJ is dissolved in PDMS, there is evidence for chain-length-dependent interpenetration of the PDMS "solvent" chains into the junction and modulation of the cybotactic region surrounding the focally located dansyl residue. Together these results demonstrate the dramatic role solvent can play in tuning the local environment that surrounds a junction in a polymer network. Future work will focus on the behavior of these systems in a tunable solvent like supercritical CO_2.

Acknowledgment. This work was generously supported by the U.S. Department of Energy.

References and Notes

(1) (a) Helfand, E. *J. Chem. Phys.* **1971**, *54*, 4651. (b) Helfand, E.; Wasserman, Z. R.; Weber, T. A. *Macromolecules* **1980**, *13*, 526. (c) Stockmayer, W. H. *Pure Appl. Chem.* **1976**, *15*, 539. (d) Yamakawa, H. *Modern Theory of Polymer Solutions*; Harper and Row: New York, 1971.

(2) Foldes, E. *Angew. Makromol. Chem.* **1998**, *262*, 65.

(3) Saltzman, W. M.; Radomsky, M. L. *Chem. Eng. Sci.* **1991**, *46*, 2429.

(4) Prasad, P. N.; Williams, D. J. *Introduction to Nonlinear Optical Effects in Molecules and Polymers*; Wiley: New York, 1991.

(5) (a) Webster, O. W. *Science* **1994**, *251*, 887. (b) Fréchet, J. M. J. *Science* **1994**, *263*, 1710. (c) Hedrick, J. L.; Miller, R. D.; Hawker, C. J.; Carter, K. R.; Volksen, W.; Yoon, D. Y.; Trollss, M. *Adv. Mater.* **1998**, *10*, 1049.

(6) Higgins, J. S.; Maconnachie, A. In *Methods of Experimental Physics*; Skold, K., Price, D. L., Eds.; Academic Press: New York, 1987; Vol. 23, Part C, p 287.

(7) (a) Heatley, F. *Prog. NMR Spectrosc.* **1979**, *13*, 47. (b) Glowinkowski, S.; Gisser, D. J.; Ediger, M. D. *Macromolecules* **1990**, *23*, 3520. (c) Schmidt-Rohr, K.; Spiess, H. W. *Multidimensional Solid-State NMR and Polymers*; Academic Press: New York, 1994.

(8) Bailey, R. T.; North, A. M.; Pethrick, R. A. *Molecular Motion in High Polymers*; Clarendon Press: Oxford, U.K., 1981; Chapter 9.

(9) (a) Mashimo, S.; Winsor, P. R. IV.; Cole, H.; Matsuo, K.; Stockmayer, W. H. *Macromolecules* **1986**, *19*, 682. (b) Adachi, K. *Macromolecules* **1990**, *23*, 1816.

(10) (a) *Dynamic Light Scattering*; Pecora, R., Ed.; Plenum: New York, 1985. (b) Chu, B. *Laser Light Scattering*, 2nd ed.; Academic: New York, 1991.

(11) (a) Valeur, B.; Monnerie, L. *J. Polym. Sci., Polym. Phys. Ed.* **1976**, *14*, 11. (b) Phillips, D. *Polymer Photophysics: Luminescence, Energy Migration, and Molecular Motion in Synthetic Polymers*; Chapman and Hall: New York, 1985. (c) Winnik, M. A. In *Photophysical and Photochemical Tools in Polymer Science*; Winnik, M. A., Ed.; Reidel: Dordrecht, The Netherlands, 1986; pp 467−494. (d) *Photophysics of Polymers*; Hoyle, C. E., Torkelson, J. M., Eds.; ACS Symposium Series; American Chemical Society: Washington, DC, 1987; Vol. 358. (e) Char, K.; Gast, A. P.; Frank, C. W. *Langmuir* **1988**, *4*, 989. (f) Sasaki, T.; Yamamoto, M. *Macromolecules* **1989**, *22*, 4009. (g) Ediger, M. D. *Annu. Rev. Phys. Chem.* **1991**, *42*, 225. (h) Waldow, D. A.; Ediger, M. D.; Yamaguchi, Y.; Matsushita, Y.; Noda, I. *Macromolecules* **1991**, *24*, 3147. (i) Németh, S.; Jao, T.-C.; Fendler, J. H. *Macromolecules* **1994**, *27*, 5449. (j) Asano, M.; Winnik, F. M.; Yamashita, T.; Horie, K. *Macromolecules* **1995**, *28*, 5861. (k) Niemeyer, E. D.; Bright, F. V. *Macromolecules* **1998**, *31*, 71. (l) Kane, M. A.; Baker, G. A.; Pandey, S.; Maziarz, E. P. III.; Hoth, D. C.; Bright, F. V. *J. Phys. Chem. B* **2000**, *104*, 8585.

(12) (a) Stein, A. D.; Hoffman, D. A.; Frank, C. W.; Fayer, M. D. *J. Chem. Phys.* **1992**, *96*, 3269. (b) Leezenberg, P. B.; Marcus, A. H.; Frank, C. W.; Fayer, M. D. *J. Phys. Chem.* **1996**, *100*, 7646.

(13) (a) Hench, L. L.; West, J. K. *Chem. Rev.* **1990**, *90*, 33. (b) Brinker, C. J.; Scherer, G. W. *Sol-Gel Science*; Academic Press: New York, 1989.

(14) (a) Parker, C. A.; Joyce, T. A. *J. Appl. Polym. Sci.* **1974**, *18*, 155. (b) Li, Y.-H.; Chan, L.-M.; Tyer, L.; Moody, R. T.; Himel, C. M.; Hercules, D. M. *J. Am. Chem. Soc.* **1975**, *97*, 3118. (c) Hoenes, G.; Hauser, M.; Pfleiderer, G. *Photochem. Photobiol.* **1986**, *43*, 133. (d) Binkert, Th.; Oberreich, J.; Meewes, M.; Nyffenegger, R.; Ricka, J. *Macromolecules* **1991**, *24*, 5806. (e) Hu, Y.; Horie, K.; Ushiki, H. *Macromolecules* **1992**, *25*, 6040. (f) Cardona, C. M.; Alvarez, J.; Kaifer, A. E.; McCarley, T. D.; Pandey, S.; Baker, G. A.; Bonzagni, N. J.; Bright, F. V. *J. Am. Chem. Soc.* **2000**, *122*, 6139.

(15) (a) Jameson, D. M.; Gratton, E.; Hall, R. D. *Appl. Spectrosc. Rev.* **1984**, *20*, 55. (b) Bright, F. V.; Betts, T. A.; Litwiler, K. S. *CRC Crit. Rev. Anal. Chem.* **1990**, *21*, 389. (c) Lakowicz, J. R.; Gryczynski, I. In *Topics in Fluorescence Spectroscopy*; Lakowicz, J. R., Ed.; Plenum Press: New York, 1991; Vol. 1, Chapter 5. (d) Steiner, R. F. In *Topics in Fluorescence Spectroscopy*; Lakowicz, J. R., Ed.; Plenum Press: New York, 1991; Vol. 2, Chapter 1. (e) Bright, F. V. *Appl. Spectrosc.* **1995**, *49*, 14A.

(16) (a) Gratton, E.; Limkeman, M.; Lakowicz, J. R.; Maliwal, B. P.; Cherek, H.; Laczko, G. *Biophys. J.* **1984**, *46*, 479. (b) Beechem, J. M.; Gratton, E.; Ameloot, M.; Knutson, J. R.; Brand, L. In *Topics in Fluorescence Spectroscopy*; Lakowicz, J. R., Ed.; Plenum Press: New York, 1991; Vol. 2, Chapter 5.

(17) (a) Munro, I.; Pecht, I.; Stryer, L. *Proc. Natl. Acad. Sci. U.S.A.* **1979**, *76*, 56. (b) Lipari, G.; Szabo, A. *Biophys. J.* **1980**, *30*, 489. (c) Quitevis, E. L.; Marcus, A. H.; Fayer, M. D. *J. Phys. Chem.* **1993**, *97*, 5762. (d) Heitz, M. P.; Bright, F. V. *Appl. Spectrosc.* **1995**, *49*, 20.

(18) Lakowicz, J. R. *Principles of Fluorescence Spectroscopy*, 2nd ed.; Plenum Press: New York, 1999; Chapters 6 and 7.

(19) Spencer, R. D.; Weber, G. *J. Chem. Phys.* **1970**, *52*, 1654.

(20) (a) Elias, H. G. In *Polymer Handbook*, 3rd ed.; Brandrup, J., Immergut, E. H., Eds.; John Wiley and Sons: New York, 1989; Vol. II, p 205. (b) Fuchs, O. In *Polymer Handbook*, 3rd ed.; Brandrup, J., Immergut, E. H., Eds.; John Wiley and Sons: New York, 1989; Vol. II, p 379. (c) Carrher, C. E. *Polymer Chemistry an Introduction*, 4th ed.; Marcel Dekker: New York, 1996.

(21) (a) Kosower, E. M. *Acc. Chem. Res.* **1982**, *15*, 259. (b) Rettig, W. *Angew Chem., Int. Ed. Engl.* **1986**, *25*, 971. (c) Reichardt, C. *Chem. Soc. Rev.* **1992**, 147.

(22) (a) Flory, P. J. *Principles of Polymer Chemistry*; Cornell University Press: Ithaca, NY, 1969. (b) *Silicon Based Polymer Science*; Ziegler, J. M., Fearon, F. W. G., Eds.; Advances in Chemistry Series 224; American Chemical Society: Washington, DC, 1990. (c) Elias, H.-G. *An Introduction to Polymer Science*; VCH: New York, 1997.

MA010013C